Determination of the Rate Parameters of N/H/O Elementary Reactions based on $H_2/O_2/NO_x$ Combustion Experiments

M. Kovács, T. Varga, C. Olm, Á. Busai, R. Pálvölgyi, I. Gy. Zsély, T. Turányi[*]

Institute of Chemistry, ELTE Eötvös Loránd University, Budapest, Hungary

Abstract

A mechanism for the description of the $H_2/O_2/NO_x$ combustion systems was optimized via the method developed in our laboratory using computer framework code *Optima++*. In total, 5073 experimental data points (ignition delay times, concentration profiles and burning velocity measurements) were collected from the literature and were reproduced using 17 recent NO_x mechanisms. The performance of the Glarborg-2018 mechanism was the best. Ten elementary reactions were selected based on local sensitivity analysis and the Arrhenius parameters of them were fitted to indirect experimental data, and direct experimental and theoretical determinations of the rate coefficients. This way more accurate rate parameters of these reactions were obtained and the temperature dependent uncertainties of the rate coefficients were calculated.

Introduction

Environmental regulations of industrial processes require the exploration of the behaviour of nitrogen oxides in combustion systems. Several detailed reaction mechanisms [1-17] were published in the last decades to describe the generation of NOx in combustion systems. These mechanisms are also applicable to facilitate the development of technologies for lowering NO_x emission from combustion systems. In a recent review, Glarborg *et al.* [1] state that for all NO_x formation routes and all major non-catalytic NO removal methods good reaction schemes are available, but the simulation results still have high uncertainty.

In this work, concentration profiles measured in jet stirred reactors, ignition delay times determined in shock tubes, concentration profiles measured in flow reactors, laminar burning velocity measurements and concentration profiles measured in burner stabilized flames (indirect measurements) related to hydrogen−oxygen combustion systems doped with NO, NO_2 or N_2O, and H_2/N_2O combustion systems were considered. These data, together with direct experimental and theoretical determinations of the rate coefficients were used to obtain the rate parameters of ten selected N/H/O elementary reactions with low uncertainty. A methodology was developed by Turányi *et al.* [18] for the determination of rate parameters based on direct and indirect measurements, and theoretical determinations. The method provides rate parameters which are in accordance with the considered indirect measurements and the literature information related to the investigated elementary reactions.

Collection of experimental data

Our aim was to collect all experimental data on hydrogen combustion influenced with nitrogen oxides related to measurements in homogenous reactors and flames. The summary of the experimental conditions and the number of the collected data is given in Table 1.

Table 1 List of the considered hydrogen combustion experiments.

Exp. type[a]	Data sets[b]	Data points[c]	T / K	p / atm	ϕ
JSR[d]	19	945	700–1150	1–10	0.1–2.5
IDT[e]	65	775	738–2712	0.14–35.9	0.3–5.0
LFR[f]	43	1538	780–1382	0.5–12.5	0.25–3.77
LBV[g]	7	88	297–299	0.197–1.02	0.15–1.79
BSF[h]	81	1727	293–970	0.026–1	0.45–1.74

[a]Exp. type: experiment type; [b]Date sets.: number of datasets; [c]Data points: number of data points; [d]JSR: concentration profiles measured in jet stirred reactors; [e]IDT: ignition delay time measured in shock tubes; [f]LFR: concentration profiles measured in laminar flow reactors; [g]LBV: laminar burning velocity measurements; [h]BSF: concentration profiles measured in burner stabilized flames

All collected indirect experimental data (5073 data points in 215 data sets of 36 experimental articles) were stored in ReSpecTh Kinetics Data (RKD) files. The RKD-format [19,20] was developed from the PrIMe kinetics data format [21,22] by adding several new keywords. These data formats are XML based and can be well read by both humans and computer codes. The RKD-format files were created with our *Optima++* code [23]. *Optima++* was also used for reading the data files, running the *FlameMaster* simulation code [24] and comparing the simulation results with the experimental data.

Table 2 Performance of the various reaction mechanisms considered at the reproduction of all experimental data and various subsets of them (see text).

Mechanism Number of data points:	E_{all} 4949	E_{filtered} 4779	E_{JSR} 945	E_{IDT} 625	E_{LFR} 1481	E_{LBV} 88	E_{BSF} 1640	E_{common} 2299
Glarborg-2018 [1]	62.20	17.50	5.57	39.98	7.04	27.93	10.52	7.54
Nakamura-2017 [2]	51.67	12.47	5.47	15.40	7.49	191.19	10.29	7.74
Zhang-2017 [3]	39.31	19.15	6.30	35.43	17.24	17.56	12.57	9.01
POLIMI-2017 [4]	65.83	18.02	17.32	32.29	9.97	37.17	11.03	17.54
Mevel-2009 [5]	89.62	75.69	4.77	146.16	10.38	-	-	23.68
Abian-2015 [6]	150.92	98.27	5.39	208.54	9.01	-	-	32.00
Klippenstein-2011 [7]	151.77	98.70	5.39	211.75	9.01	-	-	32.00
GRI3.0-1999 [8]	65.99	43.46	8.83	109.92	33.18	41.72	10.57	38.49
Okafor-2018 [9]	93.66	64.68	4.98	110.40	33.00	-	-	38.95
Song-2018 [10]	70.19	26.09	110.14	22.57	14.86	73.73	11.17	57.52
SanDiego-2014 [11]	174.27	79.42	24.11	118.41	53.46	-	-	65.31
SanDiego-2018 [12]	151.31	73.80	6.68	104.96	60.36	-	-	69.42
POLIMI-2007 [13]	181.38	116.53	6.62	233.73	26.73	-	-	73.43
Konnov-2009 [14]	143.97	124.21	13.10	182.84	104.67	-	-	98.40
Tian-2009 [15]	113.18	103.76	5.41	146.78	97.05	-	-	98.86
Rasmussen-2008 [16]	116.56	105.55	15.91	129.05	140.78	-	-	116.65
GDFKin-2016 [17]	423.52	364.64	4.31	792.71	18.04	-	-	118.23

Selection of a mechanism for the optimization

Experimental data were reproduced using detailed reaction mechanisms developed for the description of NO_x chemistry in combustion systems. 17 mechanisms listed in Table 2 were considered which are widely used in science and industry. All collected experimental data were simulated with each reaction mechanism.

The obtained simulation results, belonging to different mechanisms, were typically very different from each other and sometimes also from the experimental data. Two typical examples of the behaviour of the mechanisms can be seen on Figure 1.

Agreement of the simulation results with the experimental data was investigated comprehensively using the following objective function.

$$E(\mathbf{p}) = \frac{1}{N} \sum_{i=1}^{N} \frac{1}{N_i} \sum_{j=1}^{N_i} \left(\frac{Y_{ij}^{\text{mod}}(\mathbf{p}) - Y_{ij}^{\text{exp}}}{\sigma\left(Y_{ij}^{\text{exp}}\right)} \right)^2 \quad (1)$$

Here N is the number of datasets and N_i is the number of data points in the i-th dataset. Vector $\mathbf{p}$ contains the rate parameters. Values y_{ij}^{exp} and $\sigma\left(y_{ij}^{\text{exp}}\right)$ are the j-th data point and its standard deviation, respectively, in the i-th dataset.

The corresponding simulated (modelled) value is y_{ij}^{mod} obtained from a simulation using a detailed mechanism and an appropriate simulation method. If a measured value is characterized by absolute errors (the scatter is independent of the magnitude of y_{ij}), then $Y_{ij} = y_{ij}$. This option is used for measured concentration profiles and laminar burning velocities. If the experimental results are described by relative errors (the scatter is proportional to the value of y_{ij}), then option $Y_{ij} = \ln\left(y_{ij}\right)$ is used, which is characteristic for ignition delay time measurements and also for direct rate determinations.

We investigated the effect of filtering the influence of less reproducible experimental data. In the "filtered" calculation of the error function all experimental datasets were excluded, which provided larger than $E = 100$ values for all of the Glarborg-2018, Nakamura-2017, Zhang-2017 and POLIMI-2017 mechanisms (13 datasets were excluded out of 215). The comparison of the E_{all} and E_{filtered} columns of Table 2 shows that excluding these datasets resulted in much lower E values for most mechanisms. E_{common} is a result of a further filtering when we take into account only those datasets which have been simulated successfully with each mechanism.

Based on the results presented in Table 2, the Glarborg-2018 mechanism was selected for further investigations.
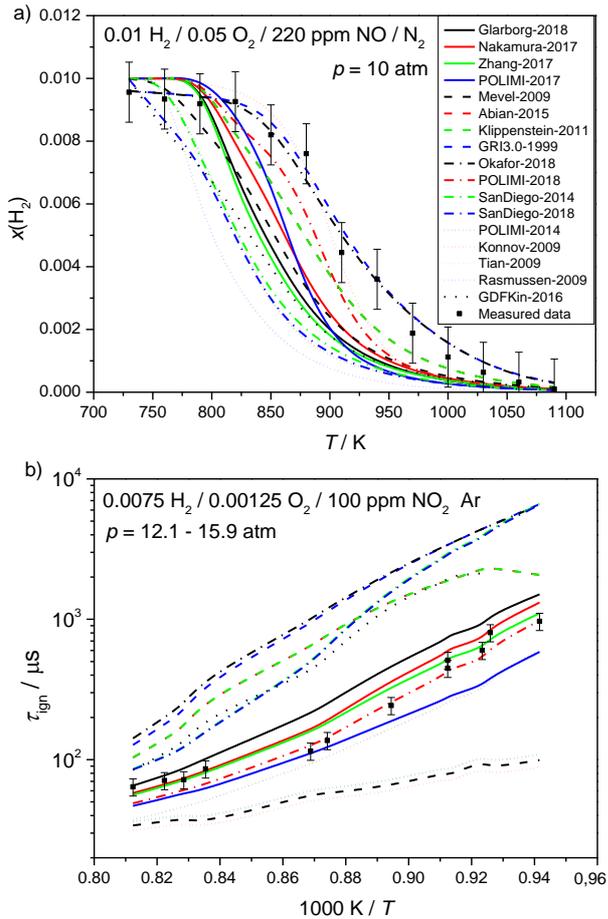
Figure 1 a) Simulation results of concentration profiles measured in jet-stirred reactor by Dayma *et al.* [25]. b) Simulation results of ignition delay times measured in shock tube by Mathieu *et al.* [26] The lines are simulation results of the corresponding mechanism shown in the label on a). The square symbols are measured data with the corresponding estimated standard deviation.

The optimisation method and results

Local sensitivity analysis was used to identify the most important elementary reactions at the conditions of the experiments. A reaction was considered important at a data point if the absolute value of the sensitivity coefficient was larger than 10% of the absolute value of the largest sensitivity coefficient. Important reactions were assigned to each dataset based on the importance of reactions at the data points. Only the important N/H/O reactions were looked for, since the rate parameters of the H/O subset have been optimised in our previous work [27]. The selected reactions are listed in Table 3. The optimal rate parameters are also shown in the table which were determined with our optimisation method described below.

The global parameter optimization method applied here has been described in detail by Turányi *et al.* [18]. The optimal set of rate parameters was obtained by the minimization of objective function Eq. (1). The optimal rate parameters were looked for in such a way that the calculated rate coefficients always remained within their prior uncertainty bands which is defined by the uncertainty coefficient Eq. (2) based on data from the NIST Chemical Kinetics Database [28], direct experiments and theoretical determinations of the rate coefficients.

$$f_{\text{prioir}}(T) = \log_{10} \frac{k_{\max}(T)}{k^0(T)} = \log_{10} \frac{k^0(T)}{k_{\min}(T)} \quad (2)$$

where $k^0(T)$ is the recommended rate coefficient, which can be considered as the mean value of the uncertainty band, $k_{\max}(T)$ and $k_{\min}(T)$ are the physically possible upper and lower limits of the rate coefficient, respectively. The determination of the uncertainty band is described in details elsewhere [29]. The determined f values are shown in Figure 2.

Table 3 List of reactions selected for optimisation and the optimised rate parameters. Units are cm³, mol, s, K. LP stands for low pressure limit.

R. number	Reaction	A	n	E/R
R1	$NO_2 + H = NO + OH$	$1.70 \cdot 10^{14}$	$-6.72 \cdot 10^{-3}$	$1.65 \cdot 10^2$
R2	$NO + HO_2 = NO_2 + OH$	$2.58 \cdot 10^{12}$	$-2.63 \cdot 10^{-2}$	$-2.12 \cdot 10^2$
R3 LP	$NO + H + M = HNO + M$	$7.47 \cdot 10^{15}$	$-1.85 \cdot 10^{-1}$	$-4.23 \cdot 10^2$
R4 LP	$N_2O + M = N_2 + O + M$	$7.36 \cdot 10^{27}$	-3.45	$3.56 \cdot 10^4$
R5	$NO_2 + H_2 = HONO + H$	$1.26 \cdot 10^4$	2.78	$1.48 \cdot 10^4$
R6 LP	$NO + O + M = NO_2 + M$	$1.07 \cdot 10^{20}$	-1.42	$1.40 \cdot 10^2$
R7	$N_2O + H = N_2 + OH$	$9.82 \cdot 10^{13}$	$-3.86 \cdot 10^{-2}$	$6.62 \cdot 10^3$
R8 LP	$NO + OH + M = HONO + M$	$5.49 \cdot 10^{21}$	-1.92	$-2.03 \cdot 10^2$
R9	$HONO + OH = NO_2 + H_2O$	$2.76 \cdot 10^{10}$	$6.70 \cdot 10^{-1}$	$-2.63 \cdot 10^2$
R10	$NO_2 + H_2 = HNO_2 + H$	$3.32 \cdot 10^2$	2.97	$1.51 \cdot 10^4$
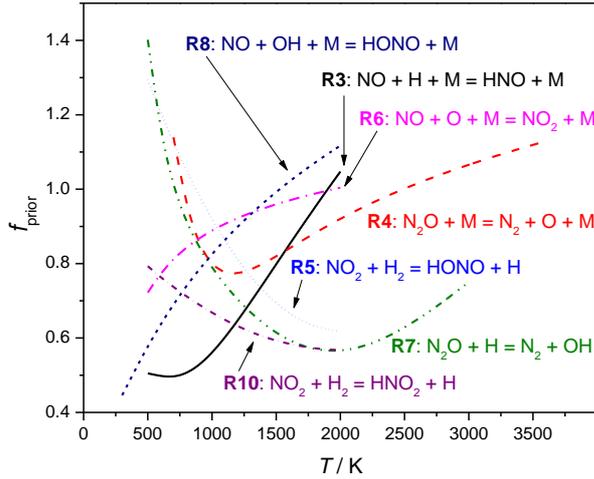
Figure 2 The temperature dependent uncertainty coefficients of the reactions identified for optimization. Three reactions out of ten have temperature independent uncertainty coefficient: R1: $NO_2 + H = NO + OH$ ($f = 0.3$); R2: $NO + HO_2 = NO_2 + OH$ ($f = 0.3$); R9: $HONO + OH = NO_2 + H_2O$ ($f = 0.6$)

The determination of the posterior covariance matrix of the optimised parameters and the calculation of the temperature dependent uncertainties of the optimised rate coefficients have been described in details in [18].

Results of this work are new recommended Arrhenius parameters of the investigated ten elementary reactions. These values are based on a large set of data (1639, 624 and 131 data points in 69, 39, 9 data sets of indirect measurements, direct measurements and theoretical determinations, respectively). Altogether 2394 data points in 117 datasets were utilized. The obtained Arrhenius parameters are given in Table 3.

Reactions R2, R6 and R7 were selected to present the initial and optimised rate coefficient – temperature functions and to compare the prior and posterior uncertainty bands. Figure 3 shows that the posterior uncertainty band of the rate coefficients obtained as a result of fitting the rate parameters to large number of data points is usually much narrower than the prior uncertainty band, obtained from processing the literature information. For most reactions the optimised rate coefficients are in good agreement with the selected direct measurements and theoretical determinations.

In order to characterize the performance of the optimized mechanism the various objective function values described above were calculated and summarized in Table 4 in comparison with the initial Glarborg-2018 mechanism. Two typical simulation results are also selected for comparison as shown in Figure 4.

Figure 3 The Arrhenius-plots of the initial and optimised rate parameters and the related prior and posterior uncertainty limits, respectively, for reactions a) R2, b) R6 and c) R7.

Table 4 The performance of the optimized reaction mechanism at the reproduction of all experimental data and various subsets of them (see text).

Mechanism	E_{all}	$E_{filtered}$	E_{JSR}	E_{IDT}	E_{LFR}	E_{LBV}	E_{BSF}	E_{common}
Number of data points:	4949	4779	945	625	1481	88	1640	2299
Glarborg-2018	62.20	17.50	5.57	39.98	7.04	27.93	10.52	7.54
Optimized	35.13	13.73	5.35	22.49	3.45	59.86	11.49	5.02
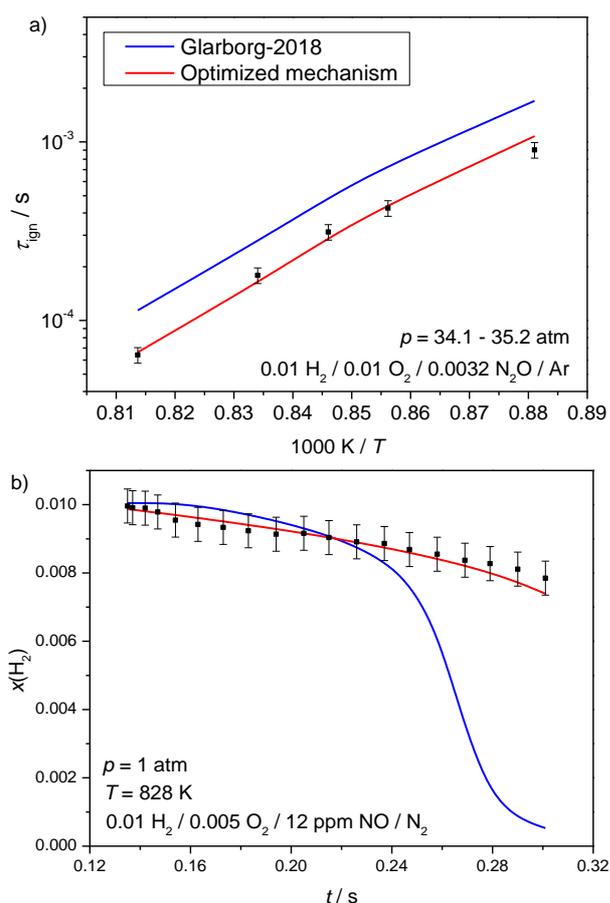
Figure 4 Comparison of the simulated results with the Glarborg-2018 and the optimized mechanism based on a) ignition delay time measured in shock tube by Mathieu *et al.* [30] and b) concentration profile measured in laminar flow reactor by Mueller *et al.* [31]

In terms of the performance of the mechanism a significant improvement was obtained based on the most informative E_{all} value (see Table 4) which decreased from 17.50 to 13.73. The simulation of the concentration profiles in laminar flow reactors gives a very good result, the experimental data were reproduced within 2σ in average. The results of the ignition delay time simulations are also improved. The optimization did not influenced as much the simulation results of the concentration profiles measured in jet-stirred reactors and burner stabilized flames, they are still with good agreement with the experimental data. The performance of the mechanism in the simulation of laminar burning velocities deteriorated due to the fact that the experimental data measured in flames have not been included to the optimization yet. This is a good further possibility to the improvement of the mechanism.

Conclusions

The performance of 17 detailed reaction mechanism describing $H_2/O_2/NO_x$ combustion systems were examined and based on their performance of simulating 5073 data points of 215 corresponding indirect experimental datasets and 775 data points of 48 corresponding datasets of direct determinations of rate coefficients. Based on this comprehensive comparison the Glarborg-2018 mechanism was found to be the actual best. The 10 most important N/H/O reaction of this mechanism were identified with local sensitivity analysis and the temperature dependent uncertainty bands of them were determined.

Rate parameters of detailed reaction mechanisms are usually based on direct measurements and theoretical determinations of the rate coefficients. These determinations typically have factor of 3 uncertainty, which corresponds to uncertainty parameter $f = 0.5$. More accurate rate coefficients, that is rate parameter values with lower uncertainty can be obtained if the results of indirect measurements are also taken into account.

With the method developed by our laboratory we carried out the optimization of the Glarborg-2018 mechanism. As a result, not only the rate coefficients were obtained with lower uncertainty, but using these new rate parameter values a more accurate detailed mechanism could be obtained for the description of this type of reaction systems.

References
[1] P. Glarborg, J.A. Miller, B. Ruscic, S.J. Klippenstein, Modeling nitrogen chemistry in combustion, Progress in Energy and Combustion Science 67 (2018) 31-68
[2] H. Nakamura, S. Hasegawa, T. Tezuka, Kinetic modeling of ammonia/air weak flames in a micro flow reactor with a controlled temperature profile, Combustion and Flame 185 (2017) 16-27
[3] Y.J. Zhang, O. Mathieu, E.L. Petersen, G. Bourque, H.J. Curran, Assessing the predictions of a NO_x kinetic mechanism on recent hydrogen and syngas experimental data, Combustion and Flame 182 (2017) 122-141
[4] T. Faravelli, POLIMI-2017 (NOx_170728), Personal communication, (2017)
[5] R. Mevel, S. Javoy, F. Lafosse, N. Chaumeix, G. Dupre, C.E. Paillard, Hydrogen-nitrous oxide delay times: Shock tube experimental study and kinetic modelling, Proceedings of the Combustion Institute 32 (2009) 359-366
[6] M. Abian, M.U. Alzueta, P. Glarborg, Formation of NO from N_2/O_2 mixtures in a flow reactor: Toward an accurate prediction of thermal NO, International Journal of Chemical Kinetics 47 (2015) 518-532
[7] S.J. Klippenstein, L.B. Harding, P. Glarborg, J.A. Miller, The role of NNH in NO formation and control, Combustion and Flame 158 (2011) 774-789
[8] G.P. Smith, D.M. Golden, M. Frenklach, N.W. Moriary, B. Eiteneer, M. Goldenberg, C.T.

Bowman, R.K. Hanson, S. Song, W.C. Gardiner, V.V. Lissianski, Z. Qin, GRI-Mech 3.0, http://www.me.berkeley.edu/gri_mech/

[9] E.C. Okafor, Y. Naito, S. Colson, A. Ichikawa, T. Kudo, A. Hayakawa, H. Kobayashi, Experimental and numerical study of the laminar burning velocity of CH4–NH3–air premixed flames, Combustion and Flame 187 (2018) 185-198

[10] Y. Song, L. Marrodán, N. Vin, O. Herbinet, E. Assaf, C. Fittschen, A. Stagni, T. Faravelli, M.U. Alzueta, F. Battin-Leclerc, The sensitizing effects of NO2 and NO on methane low temperature oxidation in a jet stirred reactor, Proceedings of the Combustion Institute (2018)

[11] San Diego Mechanism, version 2014-10-04 http://combustion.ucsd.edu

[12] San Diego Mechanism, version 2018-07-23 http://combustion.ucsd.edu

[13] A. Frassoldati, T. Faravelli, E. Ranzi, The ignition, combustion and flame structure of carbon monoxide/hydrogen mixtures. Note 1: Detailed kinetic modeling of syngas combustion also in presence of nitrogen compounds, International Journal of Hydrogen Energy 32 (2007) 3471–3485

[14] A.A. Konnov, Implementation of the NCN pathway of prompt-NO formation in the detailed reaction mechanism, Combustion and Flame 156 (2009) 2093–2105

[15] Z. Tian, Y. Li, L. Zhang, P. Glarborg, F. Qi, An experimental and kinetic modeling study of premixed NH3/CH4/O2/Ar flames at low pressure, Combustion and Flame 156 (2009) 1413-1426

[16] C.L. Rasmussen, A.E. Rasmussen, P. Glarborg, Sensitizing effects of NO_x on CH_4 oxidation at high pressure, Combustion and Flame 154 (2008) 529-545

[17] N. Lamoureux, H. El Merhubi, L. Pillier, S. de Persis, P. Desgroux, Modeling of NO formation in low pressure premixed flames, Combustion and Flame 163 (2016) 557-575

[18] T. Turányi, T. Nagy, I.Gy. Zsély, M. Cserháti, T. Varga, B.T. Szabó, I. Sedyó, P.T. Kiss, A. Zempléni, H.J. Curran, Determination of rate parameters based on both direct and indirect measurements, International Journal of Chemical Kinetics 44 (2012) 284–302

[19] T. Varga, T. Turányi, E. Czinki, T. Furtenbacher, A.G. Császár, ReSpecTh: A joint reaction kinetics, spectroscopy, and thermodynamics information system, Proceedings of the 7th European Combustion Meeting (2015) P1-04

[20] ReSpecTh webpage, http://respecth.hu

[21] M. Frenklach, Transforming Data into Knowledge - Process Informatics for Combustion Chemistry, Proceedings of the Combustion Institute 31 (2007) 125–140

[22] M. Frenklach, PrIMe Webpage, http://www.primekinetics.org/

[23] T. Varga, Á. Busai, I.Gy. Zsély, Optima++ v1.01: A general framework for performing combustion simulations and mechanism optimization (2018). http://respecth.hu

[24] H. Pitsch, FlameMaster v4.0, https://www.itv.rwth-aachen.de/

[25] G. Dayma, P. Dagaut, Effects of air contamination on the combustion of hydrogen – effect of NO and NO2 addition on hydrogen ignition and oxidation kinetics, Combustion Science and Technology 178 (2006) 1999-2024

[26] O. Mathieu, A. Levacque, E.L. Petersen, Effects of NO2 addition on hydrogen ignition behind reflected shock waves, Proceedings of the Combustion Institute 34 (2013) 633-640

[27] T. Varga, C. Olm, T. Nagy, I.G. Zsély, É. Valkó, R. Pálvölgyi, H.J. Curran, T. Turányi, Development of a joint hydrogen and syngas combustion mechanism based on an optimization approach, International Journal of Chemical Kinetics 48 (2016) 407–422

[28] J.A. Manion, R.E. Huie, R.D. Levin, D.R. Burgess Jr., V.L. Orkin, W. Tsang, W.S. McGivern, J.W. Hudgens, V.D. Knyazev, D.B. Atkinson, E. Chai, A.M. Tereza, C.-Y. Lin, T.C. Allison, W.G. Mallard, F. Westley, J.T. Herron, R.F. Hampson, D.H. Frizzell, NIST Chemical Kinetics Database, NIST Standard Reference Database 17, Version 7.0 (Web Version), Release 1.6.6, Data Version 2013.03, National Institute of Standards and Technology, Gaithersburg, Maryland, 20899-8320. , http://kinetics.nist.gov/

[29] T. Nagy, É. Valkó, I. Sedyó, I.G. Zsély, M.J. Pilling, T. Turányi, Uncertainty of the rate parameters of several important elementary reactions of the H_2 and syngas combustion systems, Combustion and Flame 162 (2015) 2059–2076

[30] O. Mathieu, A. Levacque, E.L. Petersen, Effects of N2O addition on the ignition of H_2/O_2 mixtures: Experimental and detailed kinetic modeling study, International Journal of Hydrogen Energy 37 (2012) 15393-15405

[31] M.A. Mueller, R.A. Yetter, F.L. Dryer, Flow reactor studies and kinetic modeling of the $H_2/O_2/NO_x$ and $CO/H_2O/O_2/NO_x$ reactions, International Journal of Chemical Kinetics 31 (1999) 705–724